

Multiplexing of six micro-displacement suspended-core Sagnac interferometer sensors with a Raman-Erbium fiber laser

Mikel Bravo,¹ Montserrat Fernández-Vallejo,^{1,*} Mikel Echapare,¹
Manuel López-Amo,¹ J. Kobelke,² and K. Schuster²

¹Department of Electric and Electronic Engineering, Universidad Pública de Navarra, 31006, Pamplona, Navarra, Spain

²Institute of Photonic Technology (IPHT), D-07745 Jena, Germany

*montserrat.fernandez@unavarra.es

Abstract: This work experimentally demonstrates a long-range optical fiber sensing network for the multiplexing of fiber sensors based on photonic crystal fibers. Specifically, six photonic crystal fiber sensors which are based on a Sagnac interferometer that includes a suspended-core fiber have been used. These sensors offer a high sensitivity for micro-displacement measurements. The fiber sensor network presents a ladder structure and its operation mode is based on a fiber ring laser which combines Raman and Erbium doped fiber amplification. Thus, we show the first demonstration of photonic crystal fiber sensors for remote measurement applications up to 75 km.

©2013 Optical Society of America

OCIS codes: (280.4788) Optical sensing and sensors; (060.2370) Fiber optics sensors; (290.5860) Scattering, Raman; (290.5830) Scattering, Brillouin.

References and links

1. H. Li, D. Li, and G. Song, "Recent applications of fiber optic sensors to health monitoring in civil engineering," *Eng. Structures* **26**(11), 1647–1657 (2004).
2. M. Fernandez-Vallejo and M. Lopez-Amo, "Optical fiber networks for remote fiber optic sensors," *Sensors (Basel)* **12**(4), 3929–3951 (2012).
3. S. Diaz, S. Abad, and M. Lopez-Amo, "Fiber-optic sensor active networking with distributed erbium-doped fiber and Raman amplification," *Laser Photon. Rev.* **2**(6), 480–497 (2008).
4. E. Achaerandio, S. Jarabo, S. Abad, and M. López-Amo, "New WDM amplified network for optical sensor multiplexing," *IEEE Photon. Technol. Lett.* **11**(12), 1644–1646 (1999).
5. M. Fernandez-Vallejo, S. Diaz, R. A. Perez-Herrera, D. Passaro, S. Selleri, M. A. Quintela, J. M. L. Higuera, and M. Lopez-Amo, "Resilient long-distance sensor system using a multiwavelength Raman laser," *Meas. Sci. Technol.* **21** 094017 (2010).
6. J. P. Dakin, D. J. Pratt, G. W. Bibby, and J. N. Ross, "Distributed optical fibre Raman temperature sensor using a semiconductor light source and detector," *Electron. Lett.* **21**(13), 569–570 (1985).
7. T. Kurashima, T. Horiguchi, and M. Tateda, "Distributed-temperature sensing using stimulated Brillouin scattering in optical silica fibers," *Opt. Lett.* **15**(18), 1038–1040 (1990).
8. Y. Tanaka, M. Kinoshita, A. Takahashi, and T. Kurokawa, "A wide-area sensor network based on fiber optic power supply," *Jpn. J. Appl. Phys.* **50**(11), 112501 (2011).
9. A. D. Kersey, M. A. Davis, H. J. Patrick, M. LeBlanc, K. P. Koo, C. G. Askins, M. A. Putnam, and E. J. Friebele, "Fiber grating sensors," *J. Lightwave Technol.* **15**(8), 1442–1463 (1997).
10. J. M. Lopez-Higuera, ed., *Handbook of Optical Fiber Sensing Technology* (Wiley, New York 2002), Chap. 1.
11. A. M. R. Pinto and M. Lopez-Amo, "Photonic crystal fibers for sensing applications," *J. Sens.* **2012** 598178, (2012).
12. D. Barrera, J. Villatoro, V. P. Finazzi, G. A. Cárdenas-Sevilla, V. P. Minkovich, S. Sales, and V. Pruneri, "Low-loss photonic crystal fiber interferometers for sensor networks," *J. Lightwave Technol.* **28**(24), 3542–3547 (2010).
13. G. A. Cárdenas-Sevilla, V. Finazzi, J. Villatoro, and V. Pruneri, "Photonic crystal fiber sensor array based on modes overlapping," *Opt. Express* **19**(8), 7596–7602 (2011).
14. H. Y. Fu, A. C. L. Wong, P. A. Childs, H. Y. Tam, Y. B. Liao, C. Lu, and P. K. A. Wai, "Multiplexing of polarization-maintaining photonic crystal fiber based Sagnac interferometric sensors," *Opt. Express* **17**(21), 18501–18512 (2009).

15. Q. Shi, Z. Wang, L. Jin, Y. Li, H. Zhang, F. Lu, G. Kai, and X. Dong, "A hollow-core photonic crystal fiber cavity based multiplexed Fabry-Pérot interferometric strain sensor system," *IEEE Photon. Technol. Lett.* **20**(15), 1329–1331 (2008).
 16. M. Bravo, A. M. R. Pinto, M. Lopez-Amo, J. Kobelke, and K. Schuster, "High precision micro-displacement fiber sensor through a suspended-core Sagnac interferometer," *Opt. Lett.* **37**(2), 202–204 (2012).
 17. A. M. R. Pinto, M. Bravo, M. Fernandez-Vallejo, M. Lopez-Amo, J. Kobelke, and K. Schuster, "Suspended-core fiber Sagnac combined dual-random mirror Raman fiber laser," *Opt. Express* **19**(12), 11906–11915 (2011).
 18. M. Fernandez-Vallejo, S. Rota-Rodrigo, and M. Lopez-Amo, "Remote (250 km) fiber Bragg grating multiplexing system," *Sensors (Basel)* **11**(12), 8711–8720 (2011).
-

1. Introduction

Fiber optical sensor networks can multiplex a group of sensors that are deployed either directly inside the element to be monitored or very close to it. In recent years, these networks have attracted much attention because they are a useful tool in the field of structural health monitoring, which reflects the increasing need to control the continuous conditions and to predict ongoing dangers in large infrastructures built by the human action; such as tunnels, dams, bridges, piles, pipelines, railways; or in natural events like tsunamis or geodynamical movements [1,2].

In the design of a fiber optical network diverse aspects have to be taken into account. Firstly, network topology has to be decided. In general, there are four possibilities: serial, bus, star and tree networks; each one of them showing pros and cons [2–4]. Secondly, the inclusion of optical amplification. The utilization of Er-doped fiber amplifiers (EDFA) or Raman amplification inside the network has opened up new opportunities such as the multiplexing of many sensors or the development of long-range networks. Using optical amplification, losses imposed by the passive elements and especially by the transmission channels can be compensated [3]. Furthermore, fiber optical networks based on fiber lasers structures are an attractive option because of the fact that the performance of sensor systems is enhanced considerably; in particular, they offer improved signal to noise ratio (SNR) when they are compared with the non-lasing ones due to the fact that the noise associated with the amplification is intended for the lasing process [5]. Obviously, a key element of a fiber optical sensor network is the chosen optical fiber sensor (OFS) itself. In fact, considering the kind of sensor it can be defined different types of networks such as optically powered fiber networks [6], and if the spatial distribution of the measurand is taken into account: networks based on distributed measurements using Brillouin scattering or Raman scattering [7,8] or networks with discrete measurements. This work is focused on the last one but this matter will be discussed in detail below. And finally, in addition to the purely optical technical aspects, other issues associated with the networks complexity, operational, maintenance and, last but not least, the cost must also be taking into account [3].

Up to now, the selected fiber optic sensors (FOS) for these networks are those based on conventional optical fiber such as Fiber Bragg gratings (FBGs) [9,10]. In fact, FOS show evidence of meaningful benefits when they are compared with traditional sensors such as small dimension, high sensitivity flexibility, ability to be embedded, EMI immunity, electrical isolation and, to top that, the possibility of withstanding harsh environments and being multiplexed. However, during the last years, sensors based on photonic crystal fiber (PCFs) are attracting considerable attention in the R&D activity. PCFs, characterized by a periodic arrangement of air holes running along the entire length, offer exceptional optical properties which make them appealing for optical sensing as it is thoroughly explained in [11] and references therein. So far a significant number of PCF sensors have been proposed, operating the vast majority of them as point sensors; and only a few articles can be found in the literature regarding the multiplexing of PCF optical sensors [12–15]. Q. Shi *et al.* proposed in 2008 a star topology to multiplex hollow-core photonic crystal fiber Fabry-Perot interferometric strain sensors [15]. H. Y. Fu *et al.* presented in 2009 a star and a serial configuration to multiplex Sagnac interferometric sensors based on polarization-maintaining photonic crystal fiber [14]. A year later, D. Barrera *et al.* demonstrated a serial scheme to

multiplex photonic crystal fiber interferometers sensors [12]. And, this former research group also demonstrated another serial topology to multiplex index-guiding PCF sensors [13]. The cumbersome task of multiplexing PCF sensors can be ascribed to two main reasons: firstly, the high insertion loss at each splice point between a conventional fiber and a PCF, thus the signal to noise ratio, which is a key parameter, decreases considerably; secondly, the complexity in demultiplexing and demodulating the multiplexed PCF sensing signals.

The multiplexing capability is of prime importance when real sensor networks are developed because it is possible to monitor the individual behavior of several sensors with a single interrogation unit which is the most expensive equipment. This fact considerably simplifies the sensor network and, consequently, the cost is reduced. For this reason, even though the multiplexing of PCF sensors is a demanding challenge, it is important to demonstrate valid multiplexing configurations to open up new possibilities for PCF sensors in the real market and become an alternative to their counterparts' sensors based on single mode fiber (SMF).

In this work, we propose and demonstrate a long-range sensing network that multiplex six fiber sensors based on photonic crystal fibers. The remote sensor network (up to 75 km) with a ladder or double-bus structure is based on a fiber ring laser which combines Raman and Erbium doped fiber amplification.

2. Experimental setup

The final sensor network structure is totally dependent on the kind of PCF sensor to be multiplexed. In this case, a high sensitivity micro-displacement fiber sensor using a suspended-core Sagnac interferometer, previously proposed by M. Bravo et al. [16], was chosen. Following, a brief description of the selected PCF sensing head is presented.

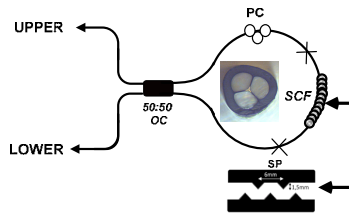


Fig. 1. Micro-displacement PCF sensing head structure.

The micro-displacement sensing head setup is depicted in Fig. 1. The Sagnac loop interferometer is formed by a 50:50 coupler, ~52 cm of a suspended-core fiber (SCF) and a polarization controller (PC). The SCF was spliced to the optical coupler (OC) output fibers (single mode fiber-SMF), having the two splices a total loss of ~3dB. The suspended-core fiber was fabricated at the IPHT (Institute of Photonic Technology, Jena, Germany) and is formed by three big holes with a diameter of ~45 μm that surround a ~6 μm diameter core (inset Fig. 1). The fiber is made of pure silica, and has a slightly triangular shape due to the asymmetry originated during the fabrication process. Stress was induced in the SCF through two stressing inducing plates (SP), shown in Fig. 1.

Light is launched through the upper port of the 50:50 OC where it is split evenly into both coupler output ports. The light travels counter propagating inside the Sagnac loop and finally interferes in the OC. Due to the high birefringence behavior of the SCF, a polarization dependence phase shift occurs which entails a variation of the interference pattern at the OC. The result of this interference is that some light is transmitted and some is reflected depending on the wavelength as it is shown in the following equation.

$$\Delta\lambda = \frac{\lambda^2}{BL} \quad (1)$$

From Eq. (1), it can be inferred that the wavelength spacing between two consecutive channels ($\Delta\lambda$) in a Sagnac loop interferometer is inversely proportional to the birefringence (B) and length of the fiber (L) [17]. On the other hand, because of the multimodal characteristics of the fiber, a propagation mode shift contributes, to a lesser extent, in the interference.

PCF sensor network

The proposed PCF remote multiplexing sensor system set-up is shown in Fig. 2. It is composed, principally, by 3 different parts: the sensor network itself, the monitoring station and the transmission channel.

The sensor network itself is based on a ladder structure. The upper path is composed of circulators whose isolation is ~ 56 dB, FBGs centered between 1544.79 nm – 1550.79 nm and having reflectivities around 96-97%, and fiber spools. The circulators redirect the reflected light from each FBG towards the PCF sensors, where it will be intensity modulated, and finally towards the lower path. It seems important to point out that the circulators isolate the reflection signal of each sensing head and force each peak to travel through the correct sensing head. For this reason, crosstalk is avoided which means that one of the most challenging issues for multiplexing interferometer sensors is addressed.

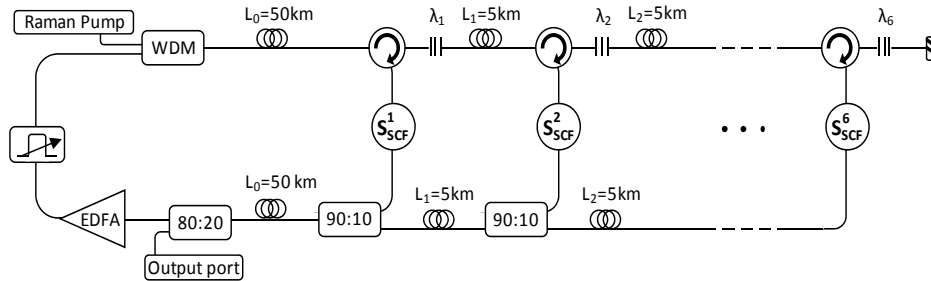


Fig. 2. Experimental set up for the proposed remote multiplexing PCF sensor system.

The purpose of the lower path is to collect each modulated sensor signal. After an empirical coupling ratio study carried out using a variable coupler, 90:10 couplers have been selected for this purpose. For performing a more realistic scheme, 5 km fiber spools have been placed between each sensing head, which simulates that each PCF sensor is placed in a different location. Thus, the distance from the first sensor to the last one is 25 km, therefore, the first PCF sensor is placed 50 km away from the monitoring station and the last one is located after 75 km.

This dual-bus PCF sensing head sensor network is connected with the monitoring station by two 50 km SMF fiber spools. One is connected to the upper path and the other to the lower one achieving an up to 75 km remote PCF sensor multiplexing network.

Finally, the network is completed by the monitoring station. It is composed by a Raman 1445 nm pump laser whose power is launched into the ring by a WDM in order to obtain Raman amplification; a programmable tunable filter (Finisar WaveShaper 1000S) which sequentially selects each FBG wavelength; a commercial EDFA and finally, an optical spectrum analyzer (OSA) that detects the output signal.

The operation mode of the system is based on a multiple cavity fiber ring laser. Each FBG creates a lasing channel which is intensity modulated by the PCF sensing head located in the upper-lower bus interconnections. Once the signals are coupled in the lower bus, an 80:20 coupler takes out 20% of light to be detected by an OSA. The rest of light is amplified by the EDFA (13 dB gain) and afterwards it is filtered with the tunable programmable filter. This filter plays two important roles: on the one hand, it selects each lasing channel and, on the other hand, it eliminates the amplified spontaneous emission (ASE) noise generated

previously by the EDFA. As the selected amplified bandwidth is limited by the narrow filter width, the Raman amplification is much more efficient.

3. Experimental results and discussion

The six PCF multiplexing sensor system is achieved by using a circulator based dual-bus sensor network. The system uses Raman-EDFA hybrid amplification to compensate the high cavity losses and thus, it is possible to achieve the lasing condition. By using the programmable tunable filter, a wavelength sweep was done to tune each FBG based laser channel wavelength.

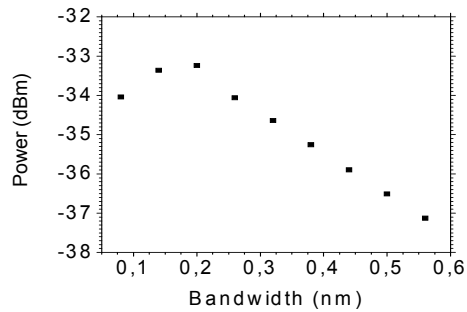


Fig. 3. Evolution of the output power vs. the filter bandwidth

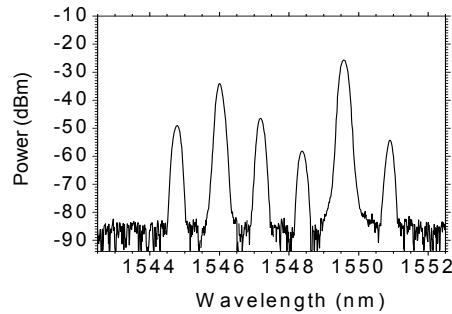


Fig. 4. Different lasing channels spectrum overview.

Raman amplification plays an essential role in the operation mode to achieve the lasing condition and the output power obtained. As M. Fernandez-Vallejo *et al.* demonstrated in [18], when the pump power increases, the lasing channel bandwidth broadens and the real problem appears when the output power is depleted. And this fact is directly related to the channel width. For this reason, a complete study of the influence of the filter width on the output power was carried out in order to reach the most efficient Raman amplification. For this purpose, the filter offers two interesting characteristics: it is possible to select the bandwidth from 40 to 0.08 nm and it is also possible to choose the filter center wavelength with a precision of 8 pm in the communications C Band (1527.4-1567.4 nm). In this work, the evolution of the output power of one of the laser emission lines in relation to the filter bandwidth has been assessed. Figure 3 shows the results. As it was expected, the narrower bandwidth, the more stimulated Brillouin scattering (SBS) spreading is observed and the broader bandwidth, the lower Raman amplification efficiency is experienced. Therefore, the optimum filter-bandwidth empirically obtained was 0.2 nm.

Taking into account that the proposed fiber ring laser does not work in multiwavelength operation, the results depicted in Fig. 4 are the combination of each lasing channel spectrum. The power difference between each peak is due to the difference of length and losses between each sensor cavity.

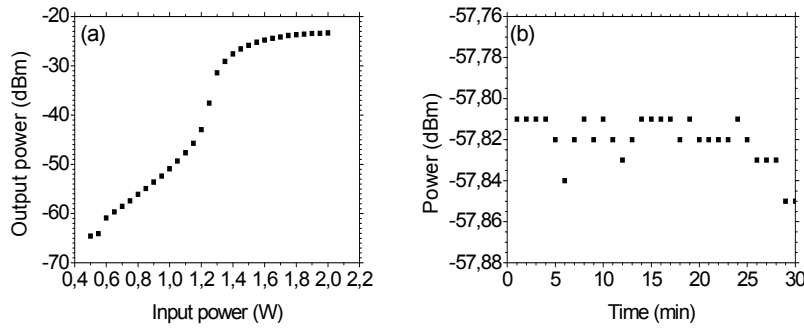


Fig. 5. Laser condition characterization and stability overview for 30 minutes.

Figure 5(a) shows the results of the study of the output power vs. the Raman pump power which demonstrates that the Raman amplification compensates the total losses of the cavity achieving the laser condition. Specifically, this plot depicts the evolution of the output power regarding the input Raman pump power for the laser channel centered at 1549.6 nm. There are two clear turning points: the first one, ~ 1.2 W, indicates that the cavity reaches the lasing threshold pump power and the second one, ~ 1.5 W, clearly suggests that the cavity reaches the saturated region. Thus, the selected Raman pump power was 1.5 W.

Taking into consideration the high influence of the instabilities in the precision of the intensity sensor interrogation, the stability of the fiber laser is a key parameter to be assessed.

Figure 5(b) provides the stability against 30 minutes time of the channel centered at 1548.44 nm whose maximum deviation is 0.04 dB. The power of this channel is the lowest which means that the worst case is being considered.

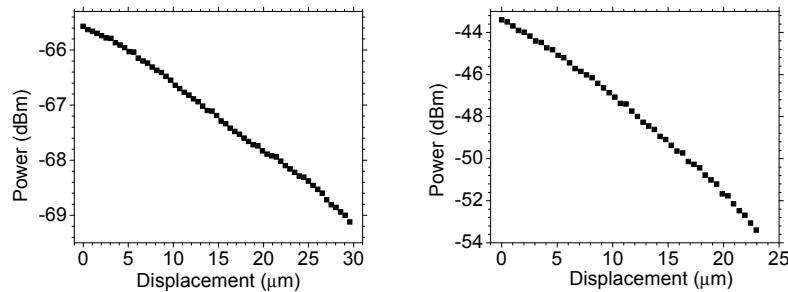


Fig. 6. PCF sensor behavior for the best (right) and the worst case (left).

To validate the behavior of the PCF sensors when they belong to the sensor network, the performance of the sensors when strain is applied has been studied. Sensitivities of 0.043 and 0.012 dBm/ μm have been obtained for the best and worst case respectively, as it is shown in Fig. 6. Both results have a very high linear fitting with a standard deviation less than 0.01. On the other hand, the repeatability of the system has been studied with a result of $\pm 0.8\%$ accuracy between consecutive sensor readings. Taking into account the 0.04 dB stability and the $\pm 0.8\%$ repeatability results, the final precision of the sensor system for the best case is $\pm 0.9 \mu\text{m}$ and in the worst case is $\pm 3 \mu\text{m}$. These results are in very good agreement with the measured data obtained when they act as point sensors in ref [16].

7. Conclusions

Six PCF sensing heads have been successfully multiplexed into an up to 75 km long remote sensor network, thus, it is the first time that the following key aspects: multiplexing of photonic crystal fiber sensors and remote measurements are merged into a fiber sensor network. This network is based on a ladder structure which operates as a fiber ring laser. A deep study of the impact of the filter width on the output power was carried out in order to

reach the most efficient system operation. The high stability of the laser ensures the correct sensor performance. Furthermore, the behavior of the multiplexed PCF sensors has been verified in the crosstalk free network. In fact, the obtained results are in good agreement with their performance when they act as isolated point sensors in a non-multiplexed interrogation system.

Acknowledgments

The authors are grateful to the Spanish Government project TEC2010-20224-C02-01 and to the European Cost Action TD-1001.